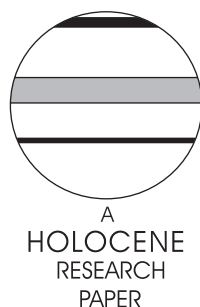


A high-resolution record of Holocene rainfall variations from the western Chinese Loess Plateau: antiphase behaviour of the African/Indian and East Asian summer monsoons

Barbara A. Maher* and Mengyu Hu

(Centre for Environmental Magnetism and Palaeomagnetism, Lancaster Environment Centre, Department of Geography, Lancaster University, Lancaster LA1 4YB, UK)

Received 1 August 2004; revised manuscript accepted 27 October 2005



Abstract: Tropical monsoons are key mechanisms for transfer of heat and moisture to higher latitudes. Here we present a high-resolution, terrestrial proxy summer monsoon record for the southeast Asian monsoon, from a rapidly accumulating Holocene loess/soil sequence in the western Chinese Loess Plateau. We use magnetic and clastic grain size proxies to make quantitative estimates of Holocene rainfall and identify variations in winter monsoon intensity. Our record reveals cyclical millennial and multimillennial rainfall changes. As with the northwest African/southwest Asian monsoon records, a short arid interval at ~ 12.5 to 11.5 ka BP (the Younger Dryas) and subsequent summer monsoon intensification are recorded. However, at 6 ka BP, the southeast Asian summer monsoon weakened, when the northwest African/southwest Asian monsoons strengthened, and then, from ~ 5 ka BP, intensified, when northwest Africa/southwest Asia became dry. These antiphase monsoonal relationships may reflect competition between sea-surface temperature changes and solar forcing. The intensity of the southeast Asian winter monsoon intensified from ~ 9 ka BP onwards, varying in its phase relationships with summer monsoon intensity. After ~ 2.25 ka BP, extreme climatic instability is indicated by both climate proxies.

Key words: Loess, palaeosols, rainfall variability, tropical climate, monsoon intensity, antiphasing, Indian monsoon, East Asian monsoon, Loess Plateau, China, Holocene.

Introduction

The major monsoon systems play a key role in transporting heat and moisture around the globe. Their impact on human populations at the present day ranges from sustenance of rain-fed agriculture to extremes of flooding or drought, affecting more than one-third of the world's population. Classically, the six major summer monsoons (of northern and southern Africa, Asia, North America, South America and northern Australasia) are thought to be driven by strong pressure gradients caused by summer heating of the continental landmasses, producing ascending air and high-level oceanward flows. Following cooling and sinking of these airmasses over the oceans, return surface flows of moisture-laden air

cross the warmed landmasses, inducing convectional instability and monsoonal rainfall. Conversely, in winter, the pressure gradient pattern is reversed, with high pressure over the cooled landmasses and low pressure over the relatively warm oceans. The intensity of the summer monsoons, and the extent of their penetration into the continents, thus varies with the strength of the land–ocean pressure gradient, as determined principally by the amount of surface heating and the temperature of the adjacent oceans (eg, Kutzbach *et al.*, 1993). For the Holocene, precession of the Earth's orbit around the Sun has caused significant changes in the seasonal distribution of surface heating. For the Northern Hemisphere, summer insolation was higher than average from ~ 15 ka BP to the mid-Holocene (peaking around 10 ka BP, at $+\sim 8\%$), and is now presently nearing its minimum as the summer solstice aligns with aphelion (eg, Berger and Loutre, 1991; Verschuren *et al.*, 2003).

*Author for correspondence (email: b.maher@lancs.ac.uk)

For the North African and southwest Asian monsoons, a wealth of proxy data has identified major northward expansion of monsoonal rainfall at the early and mid-Holocene. These data include pollen evidence for major shifts in vegetation biomes (including the ‘greening’ of the Sahara; see, eg, the COHMAP group in Wright *et al.*, 1993, for a summary), and sedimentological, biological and isotopic evidence of higher lake levels, changes in deep-sea sediment flux and increased Arabian Sea upwelling. Lake level data show that in the North African region, lacustrine deposition was initiated at ~ 14.5 ka, the onset of the ‘African Humid Period’ (eg, Street and Grove, 1979; Street-Perrott and Harrison, 1984; Gasse, 2000). A high-resolution, well-dated deep-sea record of aeolian flux (ODP Site 658C, Mauritania) substantiates both this date of onset of humid conditions (seen as a steep rise in biogenic carbonate and opal and decrease in terrigenous flux), and also a previously reported interval of aridity between ~ 12.5 and 11.5 ka BP, corresponding to the Younger Dryas (deMenocal *et al.*, 2000; Gasse *et al.*, 1990). Variations in terrigenous flux at ODP Site 658C indicate increased monsoonal intensity and precipitation from the end of the Younger Dryas to ~ 5.5 ka BP (Figure 1a), when the African Humid Period came to an abrupt end (deMenocal *et al.*, 2000). Within the Humid Period, an early Holocene interval of aridity has been identified, at ~ 8.2 ka BP (Gasse and van Campo, 1994; Alley *et al.*, 1997), marking the end of the most humid conditions in North Africa and a gradual subsequent decline in the precipitation/evaporation balance in this region (deMenocal *et al.*, 2000). However, lake-level data collated for the mid-Holocene (~ 6 ka ± 0.5 ka, eg, Jolly *et al.*, 1998) indicate conditions were still wetter than present day across North Africa, East Africa, the Arabian Peninsula, northern India and southwest China. Across this subtropical monsoonal belt, the major and abrupt shift to arid conditions has been dated to between 5 and 6 ka BP and causally associated with the ongoing decline in boreal summer insolation (eg, deMenocal *et al.*, 2000 and references therein; Gasse and van Campo, 1994).

Similar patterns in summer monsoon intensity have been recorded for the Oman/Arabian Sea and Tibetan regions. For example, Fleitmann *et al.*'s (2003) $\delta^{18}\text{O}$ record for speleothem samples from Qunf Cave, Oman indicates peak precipitation from ~ 10 to ~ 5 ka BP, with a stepped decline from ~ 8 ka BP (Figure 1b). For western Tibet, Gasse and co-workers (Gasse *et al.*, 1996; van Campo *et al.*, 1996) provide multiproxy records (pollen, radiocarbon, stable isotopes) from two sets of Holocene lake sequences (Lakes Sumxi and Bangong). They identify major strengthening of the summer monsoon at ~ 11.5 ka, with rainfall maxima from ~ 10.8 to 9.6 ka BP and ~ 8.2 to 7.2 ka BP, separated by an arid interval centred on ~ 8.8 ka BP (Figure 1c). After $\sim 6.8/13$ ka BP, the trend is towards long-term aridity. These authors thus conclude that the environmental fluctuations in western Tibet are in phase with those of North Africa.

In comparison with the North African and southwest Asian regions, relatively few long, high-resolution records have so far been reported for the southeast Asian monsoons (both winter and summer). The loess/palaeosol records of the Chinese Loess Plateau region (Figure 2) – where relatively unweathered windblown dust deposits represent relatively cool and/or dry conditions and the soils represent wetter and possibly warmer conditions – can provide natural, quasi-continuous sedimentary archives of past variations in the intensity of both the summer and winter monsoons. Because deposition of dust has continued throughout the Holocene in this region, these records can provide high-resolution information on the magnitude, timing and causes of monsoon variations through this interval. The present-day climate of the Chinese Loess Plateau is dominated by a wet, southeast summer monsoon, which delivers up to 90% of the annual precipitation. Summer heating of the Asian mountains and upland plateaux creates ascending air and high-level northwesterly airflow towards the South Pacific. As these air masses cool and sink over the ocean, a surface southeasterly flow completes the monsoonal cell; the inflowing moisture-laden air becomes unstable as it crosses the warm landmass and produces convectional rainfall. In winter, the wind directions are reversed, with high pressure over the

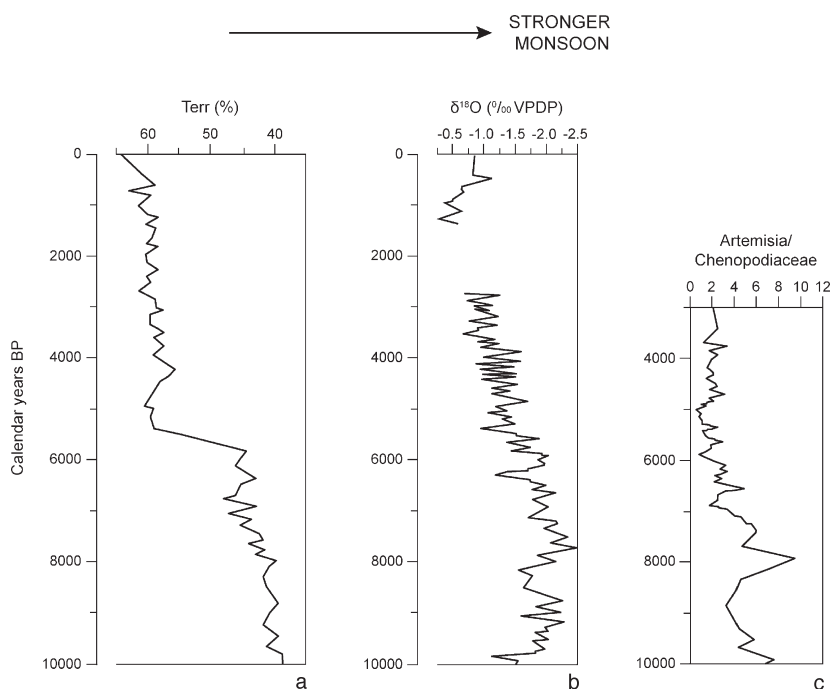


Figure 1 Summer monsoon proxy data for the Holocene interval for sites in (a) North Africa (deMenocal *et al.*, 2000), also see Figure 9c; (b) Oman (Fleitmann *et al.*, 2003), (c) West Tibet (Gasse *et al.*, 1991)

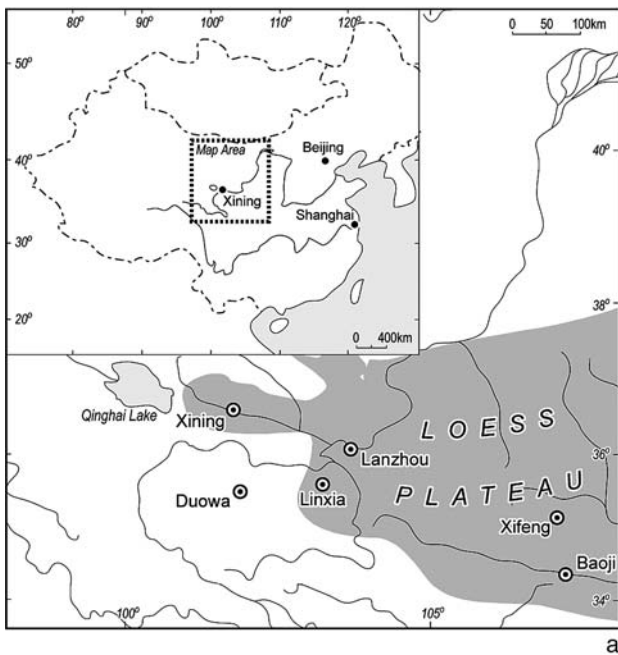


Figure 2 Location map (a), and the interbedded loess and palaeosols at the Holocene site, Duowa, western margin of the Chinese Loess Plateau (b)

continent (the Mongolian anticyclone), due to cooling and sinking of air, and low pressure over the relatively warm ocean. This winter circulation pattern creates surface northwesterly winds, bringing cold, dry airflow from Siberia. Variations in monsoon intensity affect millions of people, dependent on rain-fed farming, in this densely populated region. Earlier studies in the Loess Plateau identified a 'warm/wet' Holocene optimum, associated with complexes of palaeosols, dated (using ^{14}C methods, problematic given the likelihood of contamination by 'young' and/or 'old' carbon) to between ~ 11.5 and 5.7 calendar ka BP (eg, Zhou *et al.*, 1994). Subsequently, however, studies of higher-resolution Holocene sequences from across and beyond the Loess Plateau have indicated that this was not a period of continuous and optimum climate. Shi *et al.* (1993) reported the Holocene 'megathermal' at between 9.5 and 3.2 ka BP, with four subdivisions within it (Figure 3): a period of unstable climate from 9.5 to 8 ka BP; stable warm and wet conditions (the Holocene optimum *sensu stricto*) from 8 to 6.8 ka BP; severe and unstable conditions between 6.8 and 5.7 ka BP; and relatively warm, wet climate from 5.7 to 3.2 ka BP. Huang *et al.* (2002) have also identified, from a 4.5 -m-thick loess/soil sequence near Xi'an (southern Loess Plateau, Figure 3), a series of marked climate shifts within the Holocene. From 8.5

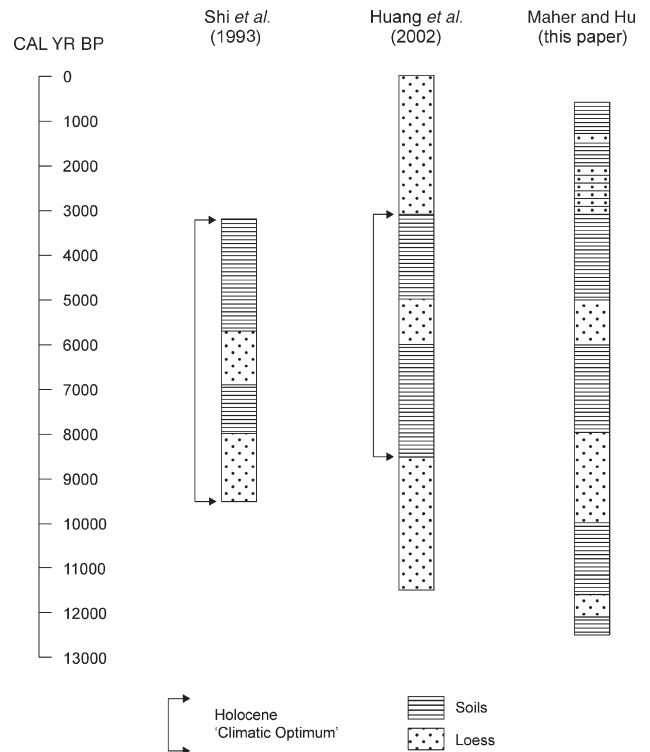


Figure 3 Holocene stratigraphies for the Chinese Loess Plateau

to 6 ka BP, soil development (producing palaeosol S_{02} , a well-developed forest soil) occurred at many locations across the Loess Plateau. However, this optimum climatic period was then interrupted by a phase of climatic aridity, between ~ 6 and 5 ka BP, resulting in burial of this soil by deposition of relatively unaltered loess. From 5 ka BP, soil formation restarted (S_{01}), indicating strengthening of the summer monsoon, until 3.1 ka BP (Pang *et al.*, 2003; Huang *et al.*, 2000, 2002), when renewed aridity is indicated by deposition of a coarser-grained loess unit (L_0). Xiao *et al.* (2002) examined a Holocene sequence, dated using AMS ^{14}C methods, at the desert/loess transition in north-central China. On the basis of organic carbon content and variations in clastic grain size, they identified dry conditions, with strong winter monsoon activity, from ~ 10 to 7 ka BP, and optimum Holocene climate (warm and wet) between 5.5 and 2.7 ka BP. They do not identify a period of desiccation from 6 to 5 ka BP but, in common with other studies, note the impact of human activities from 2.7 ka BP, associated with accelerated rates of deposition of coarse-grained loess. The possibility of asynchronicity in the timing of the Holocene climate optimum across the Chinese continent was raised by An *et al.* (2000). They suggest that peak monsoon rainfall occurred between ~ 11.5 and 9 ka BP in northeastern China, between ~ 11.5 and 7.8 ka BP in north-central China, between ~ 7.8 and 5.7 ka BP in the middle and lower reaches of the Yangtze River and around ~ 3.2 ka BP in southern China. This interpretation, dependent on robust age control and completeness of sediment stratigraphies, suggests significant weakening and southward retreat of the East Asian summer monsoon from ~ 9 ka BP.

Here, we present new climate proxy data spanning the entire Holocene period, from a ~ 5 -m-thick loess/palaeosol sequence at the western margins of the Chinese Loess Plateau, with high-resolution age control obtained by optically stimulated luminescence (OSL) dating (Roberts *et al.*, 2001). We use clastic grain size as an indicator of wind strength (ie, as a proxy for winter monsoon intensity) and a soil climofunction to estimate annual rainfall from variations in pedogenic magnetic

susceptibility (Maher and Thompson, 1995). The climofunction quantifies the direct relationship between annual rainfall and *in situ*, pedogenic magnetic susceptibility observed in modern soils. Soils that go through more wetting and drying cycles produce more of the strongly magnetic, mixed Fe(II)/Fe(III) mineral, magnetite (see, eg, Maher and Thompson, 1999, for a summary). The climofunction was originally developed in the Chinese Loess Plateau but has subsequently been validated in a region with minimal dust accumulation at the present day, the Russian steppe (Maher *et al.*, 2002a). We use the new palaeorainfall data from this western Loess Plateau site to compare with the documented sequence of Holocene monsoonal variations in the North African/Southwest Asian/West Tibet belt, and also evaluate the performance of General Circulation Model hindcasting for the mid-Holocene period (~ 6 ka).

Site, analytical methods and age control

The loess/soil sequence investigated (Figure 4), lying at an altitude of ~ 2000 m, is located at the western edge of the Chinese Loess Plateau and the eastern edge of the Qinghai Plateau, near Duowa village in Qinghai Province ($35^{\circ}25'N$; $101^{\circ}57'E$). The sediments are exposed in a terrace of the Linwusu River, a tributary of the Huang He (Yellow River). Meteorological data are not available for the site. Rainfall estimates, obtained from global climatology data sets (New *et al.*, 2000), for grid points closest to Duowa, range from 265 to 550 mm/yr. The surrounding vegetation of sparse, low-growing grasses suggests the lower estimates are appropriate. The 4.6-m-thick sequence consists of less-weathered loess units interbedded with multiple palaeosols (Figures 2–4). Nineteen samples were obtained for OSL dating (Figure 4b), with samples also taken at 5 cm intervals for magnetic and complementary analyses (particle size, carbonate, organic carbon and nitrogen). To characterize the magnetic mineralogy, concentration and magnetic grain size of the sediments, a range of magnetic measurements as made on all samples (Figure 4b): low and high frequency magnetic susceptibility (0.46 kHz and 4.6 kHz); anhysteretic remanent magnetization (normalized to the dc field used to impart the remanence); and room-temperature magnetic remanence at incremental applied dc fields of 20, 100, 300 and 1000 milliTesla (mT). Additional hysteresis (non-remnant) magnetic parameters were also obtained for each sample, including saturation magnetization, coercive force, and the ferromagnetic, paramagnetic and diamagnetic contributions to magnetic susceptibility (Maher *et al.*, 2002b). Quantitative estimates of past rainfall were made by application of a statistically derived climofunction. Following Jenny (1941), a soil climofunction is the quantitative solution of the relationship:

$$S \text{ or } S_p = f(Cl):P, R, O, T \quad (1)$$

where S , the soil, or S_p , a selected soil property, is a function of climate, with the other soil-forming variables of P (parent material), R (relief), O (organic activity) and T (time, or duration of soil formation) either effectively held constant (P , R and T) or co-varying with climate (O). The climofunction used here was generated by regression analysis of modern rainfall data (30-yr averages, AD 1951–1980) and the pedogenic susceptibility (ie, magnetic susceptibility_{B horizon} – magnetic susceptibility_{parent material}) of modern soils across the Chinese Loess Plateau and the loessic Russian steppe (Figure 5). Linear and polynomial relationships between pedogenic susceptibility

and a range of climate parameters were investigated (Maher *et al.*, 1994) but the strongest relationship ($r = +0.94$) was found for the logarithm of pedogenic susceptibility against annual rainfall:

$$\begin{aligned} \text{Rainfall mm/yr} \\ = 112 + 185 \log_{10}(\text{magnetic susceptibility}_{\text{B horizon}} \\ - \text{susceptibility}_{\text{parent material}}) \end{aligned} \quad (2)$$

The OSL and particle sizing methods and results have been reported previously (Roberts *et al.*, 2001). The OSL data show that the sequence spans the Lateglacial and entire Holocene period, the basal age being ~ 12.5 ka BP. Dust deposition appears to have been quasi-continuous through this interval. The dust accumulation rate was lowest from ~ 12 to ~ 2.5 ka BP, at ~ 20 cm/kyr, increasing to ~ 34 cm/kyr at ~ 2.5 ka BP and then to 80 cm/kyr from 0.68 ka BP to the present day (Roberts *et al.*, 2001). The upper ~ 1.3 m of the section have been subjected to significant human disturbance, as indicated by the OSL, particle size and magnetic data, and so will not be used here for palaeoclimatic reconstruction.

To apply the magnetic susceptibility/rainfall climofunction, it has to be shown that climate is the key factor influencing the *in situ*, pedogenic susceptibility. For these loess/palaeosol sequences, other soil-forming factors are either effectively constant (relief and parent material) or co-vary with climate (organic activity). The potential confounding factor is time, that is, the duration of formation of each of the soil units. Here, the OSL dating enables calculation of the soil-forming durations for each of the palaeosols. No correlation is observable between soil-forming duration and degree of soil development (Figure 6). Indeed, it is notable that the most mature palaeosols formed when rates of dust accumulation were higher, rather than lower. These data demonstrate that the degree of soil development at this site (as indicated by variations in organic carbon and nitrogen, magnetic susceptibility and inorganic carbonate, all of which are strongly correlated, Figure 4b) is not significantly influenced by changes in sedimentation rate. Thus, climate (and especially, rainfall) appears to be the major influence on soil properties, including soil magnetic properties. Hence, the statistically derived relationship between modern rainfall and the pedogenic susceptibility of modern loessic soils (from both the Chinese Loess Plateau and the Russian steppe, Figure 5) can be used to reconstruct past rainfall variations from the pedogenic susceptibility values of the Holocene palaeosols at Duowa.

For reconstruction of winter monsoon intensity, we follow, eg, Xiao *et al.* (2002) and use variations in the clastic grain size as a proxy for wind speed and hence winter monsoon strength. The median grain size, and the percentage of particles $> 40 \mu\text{m}$, are two commonly used parameters in this context, with shifts to higher values reflecting enhanced aeolian transport of coarser particles.

Results

Figure 7 (a and b) shows the reconstructed rainfall and clastic grain size data for this site through the Holocene. For rainfall, the estimated values vary by a factor of ~ 5 , from a minimum of ~ 70 mm/yr to ~ 375 mm/yr. The coarse grain percentage varies by a factor of ~ 7 , with maximum values associated with the late Holocene interval, from ~ 2.5 ka BP onwards. The median grain size shows an overall increase from the early Holocene (~ 9 ka BP) onwards (Figure 8).

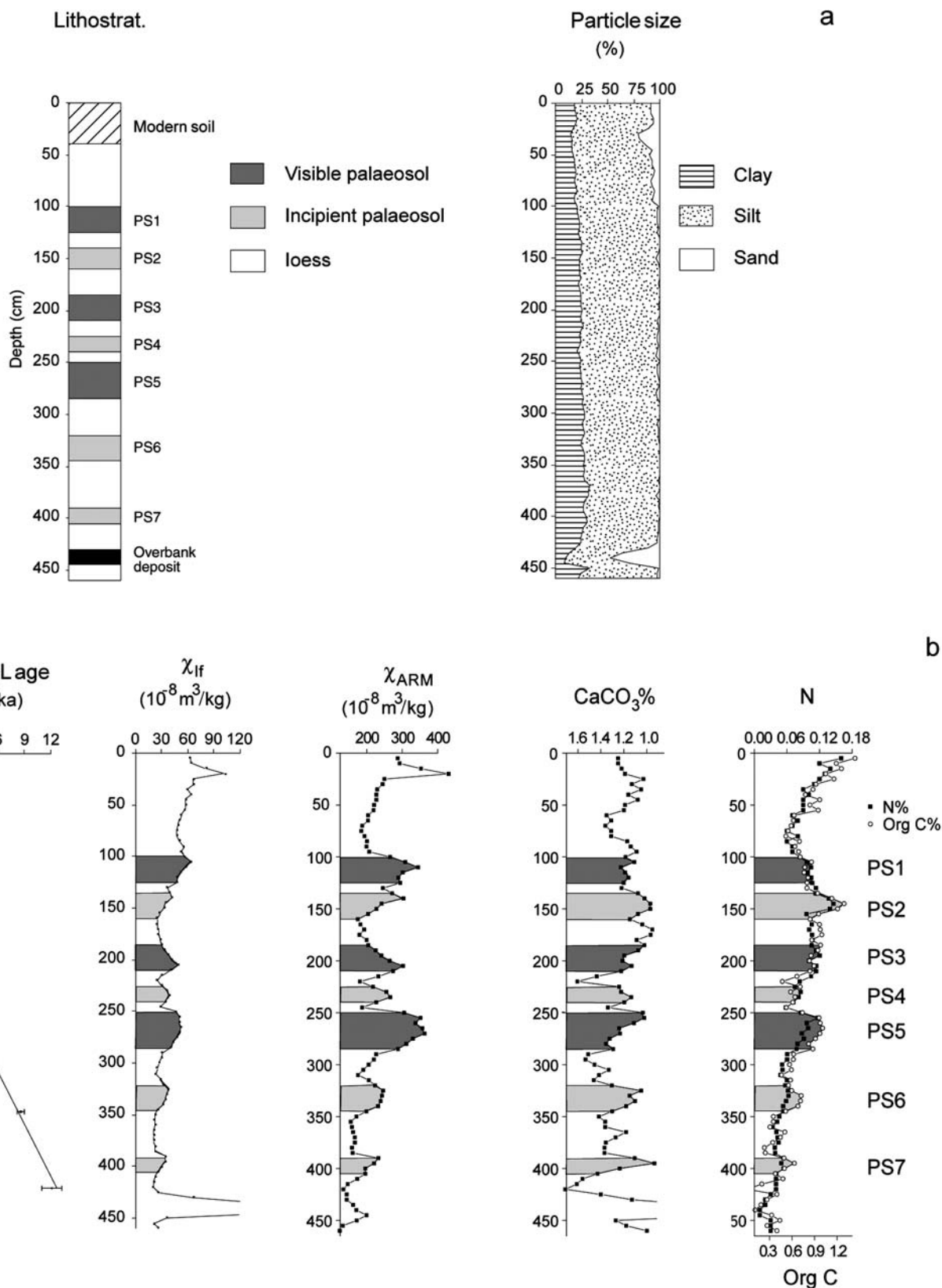


Figure 4 (a) Stratigraphy and particle size, and (b) OSL dating, magnetic and carbon, nitrogen and calcium carbonate data for the loess/soil sequence at Duowa, Qinghai Province (35°25' N; 101°57' E), from Maher *et al.* (2002b)

The rainfall data indicate that postglacial conditions were established in two distinct steps. Moderate precipitation values prior to ~12.5 ka BP were succeeded by an abrupt return to arid conditions, for a period lasting ~1 kyr. This period of desiccation was associated at its inception with intense winter monsoon winds (as indicated by high values of the grain size proxy). From ~11.5 ka BP, the start of the Holocene,

precipitation values recovered rapidly, and wind speeds decreased – but only until ~10 ka BP when precipitation declined to its Holocene minimum value, for an interval lasting ~2.5 ka. For this interval, ie, from ~10 to 7.5 ka BP, the intensities of both the summer and winter monsoon appear to have diminished and then begun to recover; the clastic grain size proxy shows variable but generally low values during

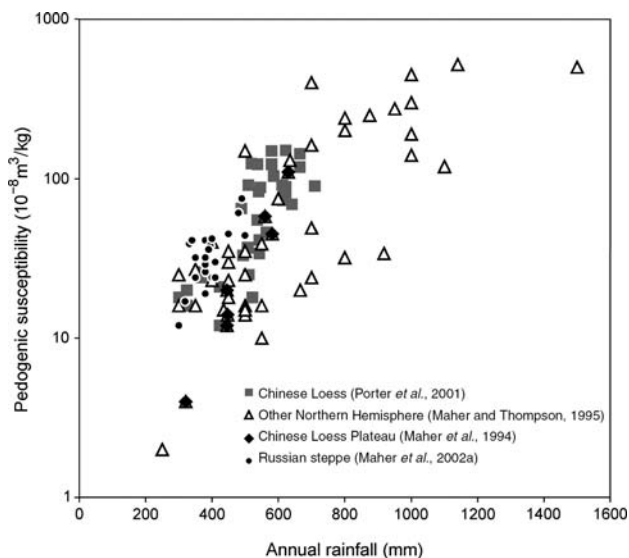


Figure 5 Derivation of the magnetic susceptibility climofunction: the rainfall/pedogenic magnetic susceptibility training set (from Maher *et al.*, 2002a)

this interval. From ~ 7.5 to 6 ka BP, rainfall values then steadily increased, to reconstructed precipitation values of 250–350 mm/yr, in coincidence with (a slightly lagging) increase in values of the winter monsoon grain size proxy. From ~ 6 to 5 ka BP, rainfall declined once more and winter monsoon strength also appears to have decreased at this time. From ~ 5 to 2.6 ka BP, rainfall levels recovered to reach their highest Holocene levels, at close to 400 mm/yr. Again, winter monsoon intensity also appears to have increased in tandem through this humid interval.

The late Holocene period, from 2.6 ka BP, appears marked by exceptional climate instability, with rainfall varying by more than 50% and clastic grain size also displaying rapid and large shifts. Humid periods appear centred on ~ 2.4 ka BP, 2 ka BP and 1 ka BP, and arid periods on ~ 2.2 and 1.5 ka BP. In this latter part of the record, the direct relationship between rainfall and winter monsoon strength, apparent from ~ 7.5 ka BP onwards, appears to have inverted; from ~ 2.6 ka BP onwards, periods of enhanced summer monsoon activity appear to have been associated with reduced winter monsoon intensity. Spectral analyses were performed, using the package Analy-series 1.2 (Paillard *et al.*, 1996), sampling the data at 200 yr intervals. Singular Spectrum Analysis (Paillard *et al.*, 1996; Ghil, 2002) highlights the signal/noise and reveals cyclical oscillations in the rainfall data with a possible dominant periodicity at 3.49 kyr (but with the caveat that the entire record is only 12.5 kyrs in duration). Finally, the median clastic grain size (Figure 8), which has varied throughout the Holocene, displays an overall trend to increased values from ~ 9 ka to the present day, suggesting increased wind intensities and/or an increase in source particle size throughout this entire interval. Time series analyses of the median grain size data, as described above, reveal possible cyclicities at ~ 5 kyr (caveat as above) and 1.75 kyr.

Discussion

This high-resolution, well-dated sedimentary sequence from the western margins of the Chinese Loess Plateau provides the most complete record yet for this region of Holocene variations in summer and winter monsoon activity. It reveals

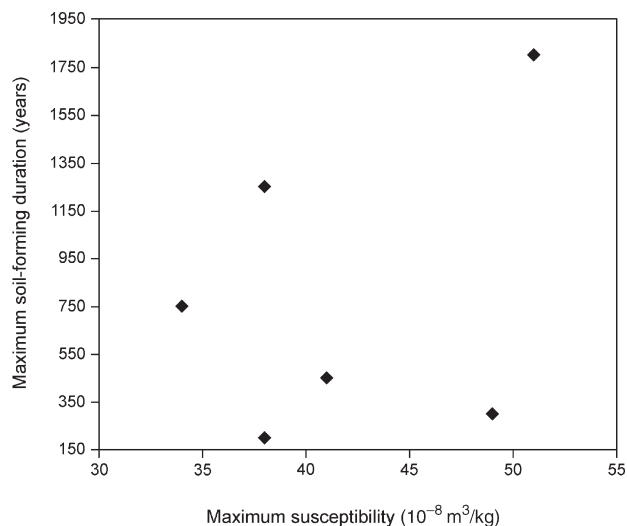


Figure 6 Soil development (as indicated by *in situ*, pedogenic magnetic susceptibility) versus soil-forming duration, Duowa palaeosols

alternating and abrupt phases of humidity and desiccation at sub-Milankovitch frequencies throughout the Holocene period. Such millennial and submillennial cyclicities, which appear almost ubiquitous in Holocene sequences across both hemispheres, are linked most often with solar forcing and changes in ocean circulation (eg, Stuiver *et al.*, 1997; Bond *et al.*, 2001). The concept of a ‘mid-Holocene climatic optimum’ or ‘Mega-thermal’ is overturned, given the evidence for three successive humid periods between ~ 11.5 and 10 ka BP, ~ 8 and 6.5 ka BP, and ~ 5 and 2.5 ka BP (the most humid phase of the three). The wetter phases were interspersed by significant intervals of aridity, including one from ~ 12.5 to 11.5 ka BP, from ~ 10 to 8 ka BP and one at the mid-Holocene (~ 6 to 5 ka BP). It is tempting to correlate the 1-kyr period of renewed post-glacial aridity between ~ 12.5 and 11.5 ka BP with the Younger Dryas, as also experienced by the North African monsoonal region (eg, deMenocal *et al.*, 2000). The age uncertainties at this part of the sequence render such correlation tentative, however. The significance of the mid-Holocene desiccation is discussed below. From ~ 2.5 ka BP onwards, climatic and environmental instability is indicated by both our rainfall and wind speed proxies.

The sequence of monsoon events recorded at Duowa extends and agrees with (Figure 3) the southern Loess Plateau records reported by Huang and co-workers (Pang *et al.*, 2003; Huang *et al.*, 2000, 2002). Similarly complex Holocene climatic variations – ie, successive humid phases and marked instability from ~ 2.5 ka BP – have also been reported by, eg, Rhodes *et al.* (1996), from multiproxy analysis of sediment cores from Lake Manas, northern Xinjiang (dated by radiocarbon methods), Zhang *et al.* (2000), for a fluvial sequence from the southern Tengger Desert (northwest China) and Xiao *et al.* (2002) for a site at the loess/desert transition in north central China. Morrill *et al.*'s (2003) synthesis of a number of Asian Holocene monsoon records also reveals some broad-scale and abrupt monsoonal changes, notably the increase in summer monsoon intensity at ~ 11.5 ka BP, which is recorded across both the southwest and southeast Asian monsoon zones. This major enhancement of the southeast Asian monsoon coincides with the start of the Holocene, with major reorganizations of climate across many regions of the world. Global teleconnections, both zonal and meridional, have been invoked to account for these near-synchronous and large changes, with

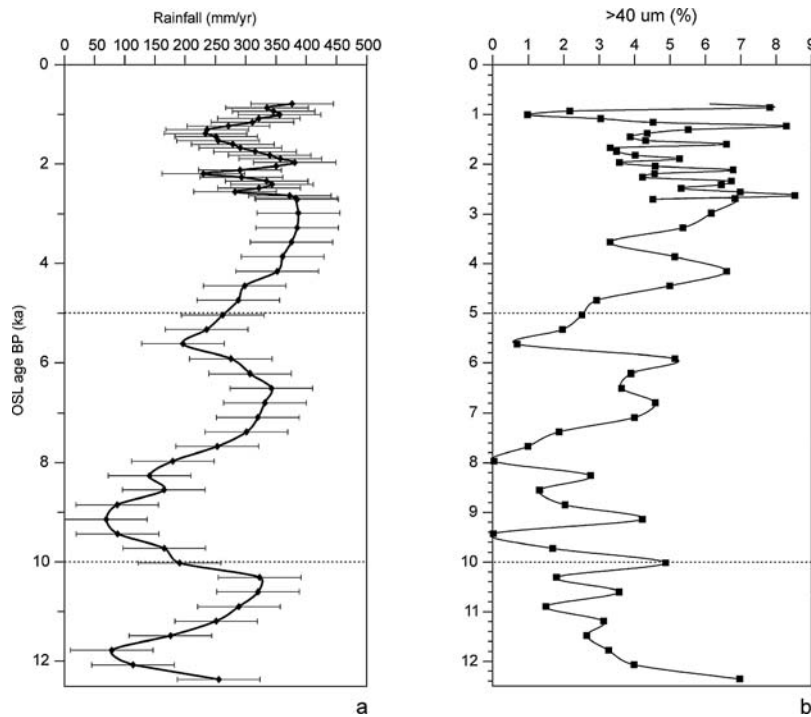


Figure 7 (a) Record of rainfall at the Duowa site through the Holocene (reconstructed using the soil magnetism/rainfall climofunction) and (b) variations in clastic grain size. Prior to insertion into the rainfall climofunction, the palaeosol susceptibility data were corrected first for the contents of calcium carbonate and organic carbon and nitrogen (effective dilutants of the magnetic susceptibility signal)

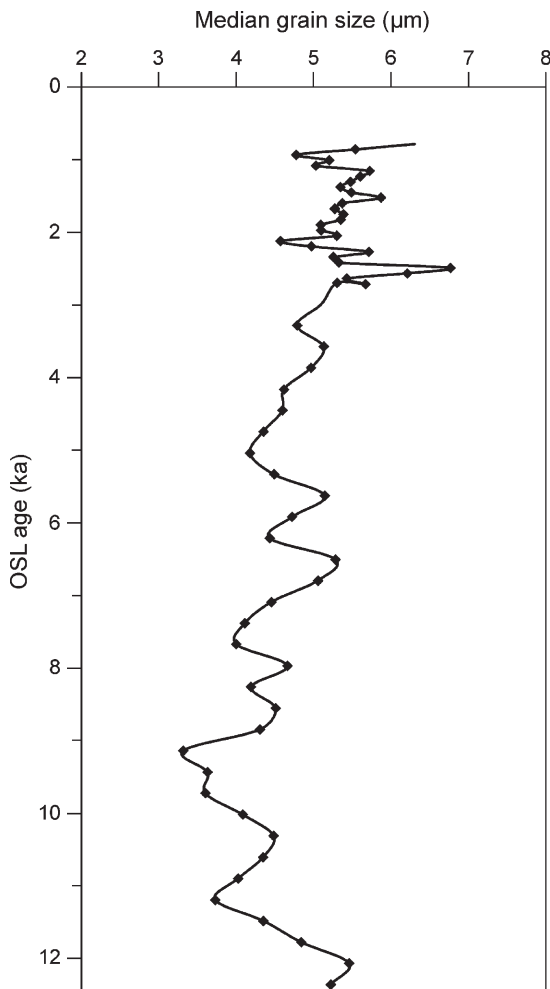


Figure 8 Variations in the median clastic grain size at Douwa through the Holocene interval

causal links suggested between changes in deep water formation in the North Atlantic and changes in the Asian monsoon system (eg, Overpeck *et al.*, 1996). At the mid-Holocene, the period of desiccation recorded by Morrill *et al.* is dated (by radiocarbon methods) to ~ 4.5 – 5 ka BP, rather than the interval identified here at ~ 6 – 5 ka BP. Comparison of the Duowa record with the South China Sea reconstruction of Wang *et al.* (1999) also reveals reasonable agreement (with the exception of the period from ~ 10 to ~ 8 ka, when the offshore record suggests an extended period of humid conditions in contrast to the desiccation recorded at Duowa). Detailed evaluation of possible synchronicity between all these records is difficult at present because of the variable quality of the dating control. In general, there seems to be strong agreement across the northern and north-central Chinese region for a period of cold, dry climatic conditions from ~ 10 to 8 ka BP, warmer and wetter conditions from ~ 8 to 6 ka BP, and most humid conditions from ~ 5 to 2.5 ka BP. Independent biological and geomorphological evidence exists for enhanced summer monsoon activity at ~ 8 – 6 ka BP, with significant northward shifts in the range of elephant, giant panda and bamboo (Winkler and Wang, 1993) and major palaeoflood deposits in the middle reaches of the Huang He (Yellow River, Yang *et al.*, 2000). At 8.2 ka BP, a short-lived episode of cooling in Greenland and aridification in subtropical North Africa has been reported (eg, Alley *et al.*, 1997; Gasse and van Campo, 1994). Given the error bars, it is not possible to identify any significant rainfall change in the Duowa record at this time.

Earlier inferences of a continuously humid, mid-Holocene climatic optimum (ie, from ~ 7 to ~ 2.5 ka BP) are confounded by the presence at Duowa, and other suitably high sedimentation rate sites, of a relatively unweathered loess unit above the middle Holocene palaeosol (Figure 3). At Duowa, this loess unit represents a ~ 1 kyr interval of desiccation, from ~ 6 to 5 ka BP. The early and mid-Holocene is characterized in the North African/Arabian Sea/Western Tibet monsoonal belt

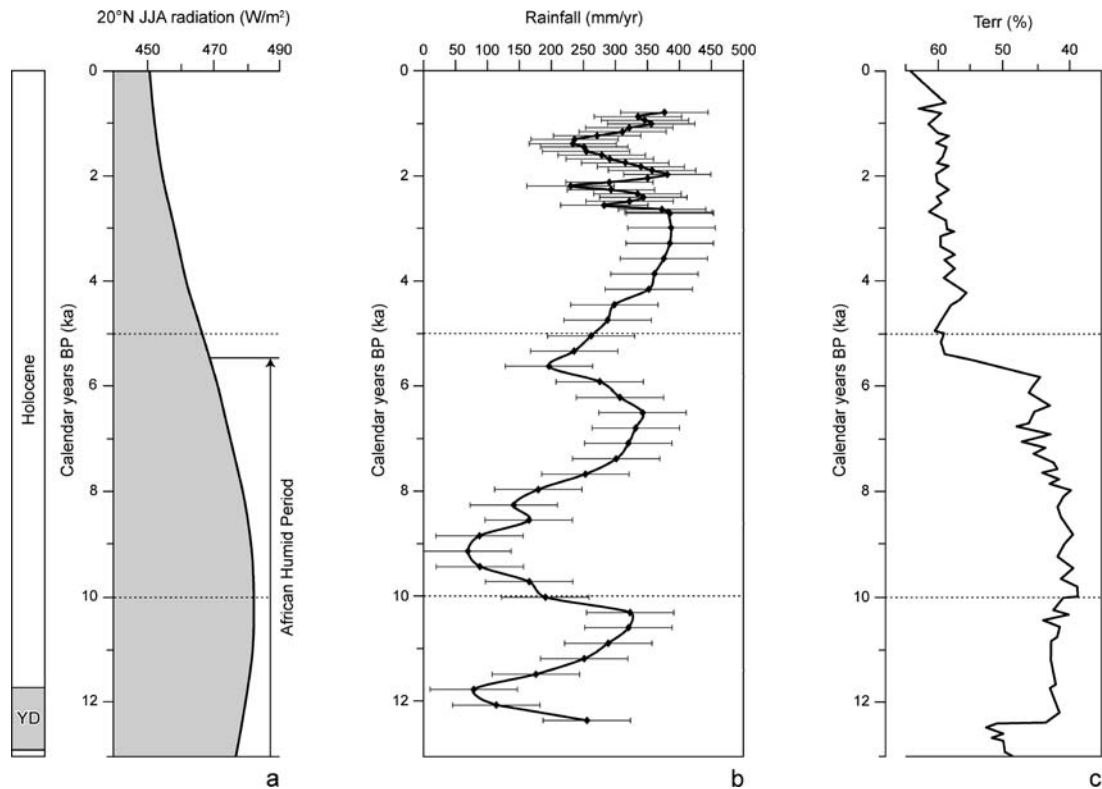


Figure 9 (a) Northern Hemisphere summer (June, July, August) insolation curve, calculated for 20°N (Berger and Loutre, 1991), spanning the Younger Dryas chronozone and the succeeding Holocene interglacial stage. (b) Reconstructed annual rainfall record from Duowa (from the soil magnetism/rainfall climofunction, ± 1 SE). (c) Record of terrigenous dust input to a deep-sea sediment site off the west African coast (ODP Site 658C, off Mauritania; deMenocal *et al.*, 2000). High terrigenous dust concentrations reflect increased aridity in northwest Africa

as a period of enhanced summer monsoon intensity, associated with enhanced Northern Hemisphere, summer insolation (Figure 9a). Recent work on palaeoclimate models run for this time interval (eg, within the palaeoclimate intercomparison modelling project, PMIP) confirms that the orbitally induced enhancement of Northern Hemisphere summer insolation at 6 ± 0.5 ka BP resulted in northward displacement of the ITCZ and hence of the monsoon front over northern Africa, while the enhanced land–sea contrast increased the flux of moisture from the ocean to the continent (Harrison *et al.*, 1998; Joussaume *et al.*, 1999). Indeed, all the PMIP models consistently underestimate the extent of the northward shift in the monsoon front (as recorded by the palaeo-lake level data). Changes in sea-surface temperatures (SSTs) and vegetation cover, as well as the orbital forcing, are required in order to approach the observed African monsoon intensity (eg, Texier *et al.*, 2000). In contrast with both the palaeoenvironmental data for the North African/southwest Asian/Western Tibet belt and the majority of the PMIP results, our reconstructed Holocene rainfall record (and its agreement with other collated data for the north-central China region) suggests that the intensity of the east Asian summer monsoon was diminished, rather than enhanced, at 6 ka BP. Of the PMIP models, only the MRI2 model (eg, Kitoh and Murakami, 2002) hindcasts desiccation in this region at this time. (However, in this model, the reduction in the hydrological cycle reflects increased evaporation rather than decreased precipitation.) Given enhanced boreal summer insolation at this time, and the overwhelming evidence for monsoon intensification in the African and southwest Asian monsoons, why would the Chinese Loess Plateau have experienced a weaker summer monsoon? Regional land/sea geography may be key, as increased summer insolation, expected to increase monsoon intensity, may have

been countered by reduced land–ocean contrast resulting from warmed sea-surface temperatures (SSTs). In model experiments run at 9 ky BP and 6 ky BP, the orbital forcing (with modern SSTs) increased monsoon intensity by $\sim 30\%$ and $\sim 18\%$, respectively, with increased precipitation values in the monsoon zone ($0\text{--}40^\circ\text{N}$, $50\text{--}120^\circ\text{E}$) of $\sim 6\%$ and $\sim 5\%$ (Basil and Bush, 2001). Adding warm, El Niño-like SSTs in the central and eastern Pacific, however, resulted in reductions in the Asian land–ocean thermal gradient and the east–west Pacific pressure gradient. Weakening of the Asian monsoon winds thus ensued; precipitation reduced by $\sim -5\%$ in the 9 ky BP simulation and $\sim -6\%$ at 6 ky BP. In contrast, for North Africa, the monsoon response to these two sets of forcings was dominated by insolation enhancement and the warm Pacific SSTs reinforced, rather than weakened, the African monsoon. Similarly, Texier *et al.* (2000) ran sensitivity studies with prescribed forcings inferred from the palaeodata: the first with enhanced SSTs in the Bay of Bengal and South China Sea; the second with the modern Sahara desert replaced with xerophytic woodland and grassland. In both cases, the degree of inland penetration of monsoon rain in the Asian region was reduced. However, in the case of the green Sahara, a shift in the position of the major large-scale convergence area enhanced the precipitation in India. Liu *et al.* (2004), running a fully coupled AGCM, also identify the key influence of ocean feedbacks in diminishing the intensity of the Asian monsoon at the mid-Holocene. In spatial terms, however, there remains a palaeodata/model mismatch, as these authors report reduced precipitation only in eastern China, with increased precipitation in the central region (in contrast to the desiccation recorded at our Holocene site).

After ~ 6 ka BP, the rainfall pattern seen at Duowa is again directly opposite to that observed for the North African/

Southwest Asian/West Tibet belt, where palaeodata indicate increasing desiccation after ~ 6 ka BP (Figure 9c). In China, our reconstructed rainfall record shows increasing values, reaching a Holocene peak (~ 375 mm/yr) at ~ 3 ka BP (Figure 9b). Tropical South America also appears to have experienced a major, synchronous change to higher precipitation from about 4 ka BP (Nuñez *et al.*, 2002; Marchant and Hooghiemstra, 2004). These changes have taken place as Northern Hemisphere summer insolation has decreased (and is now presently nearing its minimum as the summer solstice aligns with aphelion, Figure 9a). From ~ 2.5 ka BP, the Chinese record is marked by rapid and large shifts in both summer and winter monsoon intensity, but with wetter phases centred on ~ 2.2 ka, 2 ka and 1 ka. This consistently antiphase relationship between the Loess Plateau record and the North African/Indian/Western Tibet records substantiates model studies that identify internal feedbacks, especially SST variations, as a key feedback in modulating the response of the East Asian monsoon to orbital forcing. Liu *et al.* (2004) note the modelled effect of the Asian winter monsoon on the austral summer monsoon; intensification of the Asian winter monsoon lowers SSTs in the South China Sea and northern Indian Ocean, thus increasing surface pressure gradients and the strength of northerly winds towards the Southern Hemisphere. Further interaction between the Northern and Southern Hemispheres may have resulted from shifts in latitudinal thermal gradients driven by cyclical El Niño–Southern Oscillation (ENSO) events (Turney *et al.*, 2004). Palaeo-ENSO records for the tropical eastern Pacific indicate the onset of modern ENSO periodicities around 5 ka BP (eg, Moy *et al.*, 2002; Gagan *et al.*, 2004), with an abrupt increase in ENSO magnitude ~ 3 ka BP, and subsequent decline from ~ 1.2 ka BP. The nature and direction of interactions between the Asian monsoon and ENSO events remain to be resolved. Yang (1996), for example, suggests that zonal displacement of areas of warmed SSTs in the central and eastern equatorial Pacific, associated with strong ENSO events, could have shifted surface convergence and convection further to the east, possibly weakening the Asian monsoon. Conversely, according to Liu *et al.* (2000), monsoon intensification in the early and mid-Holocene may have inhibited development of warm ENSO events through enhancement of trade winds in the equatorial Pacific.

Conclusions

(1) A new, high-resolution, well-dated summer monsoon record from the western margins of the Chinese Loess Plateau shows that there were rapid (sub-Milankovitch) alternations between arid and humid phases through the Holocene.

(2) Millennial-scale variations are also apparent in the proxy record (percent of particles >40 μm) of winter monsoon intensity, with significant cyclicity at ~ 5 kyr and 1.75 kyr. From ~ 12 to 7.5 ka BP, there is an overall trend to reduced wind intensity, out of phase with summer monsoon intensity through this interval. From ~ 7.5 to ~ 2.5 ka BP, winter monsoon intensity is more variable and appears in-phase with the summer monsoon variations. From ~ 2.5 ka BP onwards, the grain size (and rainfall) data indicate extreme climatic variability. On the basis of the median grain size variations, a trend to increasing median size is observable from ~ 9 ka onwards, suggesting either stronger winter monsoon winds and/or a change in the particle size of the sediment source. The results indicate decoupling of the Southeast Asian winter and

summer monsoons, reflecting operation of separate forcing mechanisms for the two phenomena.

(3) Rather than a continuous ‘mid-Holocene climatic optimum’, the Duowa site records three humid intervals, from ~ 11.5 to 10 ka BP, ~ 8 to 6 ka BP and, the wettest phase, from ~ 5 to 2.4 ka BP. A short period of aridity from ~ 12.5 to 11.5 ka BP, also associated with a strengthened winter monsoon, may be correlative with the Younger Dryas. After this interval of aridity, summer monsoon intensity increased rapidly and markedly. The mid-Holocene interval, ~ 6 to 5 ka BP, is marked by weakening of the summer monsoon rather than intensification.

(4) This record, which is in agreement with other Holocene records from the region, appears consistently antiphase with Holocene summer monsoon records from the North African/Arabian/Indian/Western Tibet monsoonal belt (all of which appear in-phase with each other).

(5) Published palaeodata and modelling studies indicate that intensification of the North African and Southwest summer monsoons during the early to mid-Holocene period was causally related to enhanced boreal summer insolation from orbital forcing, amplified by vegetation and SST feedbacks. In contrast, given the antiphase behaviour recorded here, the East Asian monsoon appears to be dominated by the modulating effects of warmed SSTs in the West Pacific/South China Sea, which so weaken the inflowing surface winds that inland penetration of monsoonal rain is significantly reduced. Of the published mid-Holocene GCM data sets, only two models hindcast desiccation for the East Asian region at this time (the MRI, Kitoh and Murakami, 2002 and FOAM, Liu *et al.*, 2004). Of these, FOAM identifies reduced precipitation but for the eastern/coastal Chinese area rather than the north/central/inland area represented by the Duowa record.

(6) The consistently antiphase relationship between this southeast Asian monsoon record and the North African/Indian/west Tibet records indicates that internal feedbacks, probably involving SST variations and possibly related to/interacting with the mid-Holocene onset of strong ENSO events, are a key modulator of the southeast Asian monsoon response to precessional orbital forcing. If ongoing, the rapidity and magnitude of monsoonal changes identified within the last ~ 3.5 ka, possibly driven by solar output variations, will have major effects through climate teleconnections across the globe, with extreme societal implications for the large human populations in this region, given that existing water resource and agricultural systems are based on relatively wet, but apparently unreliable, southeast Asian summer monsoons. Model simulations that fail to capture the Holocene antiphasing of these major monsoon systems may require enhanced regional parameterisation to resolve the land/sea interactions in this region, in order to make robust predictions of future monsoonal changes.

Acknowledgements

We are grateful to Prof. Ann Wintle and Dr Helen Roberts, who both collaborated in fieldwork and performed the OSL dating in this project, Prof. Han Jiamo and Drs. Lu Houyuan, Wu Naiqin, and Yin Gongming for assistance with fieldwork sampling, Phil Barker for helpful comments and Frank Oldfield for his thoughtful review. BAM was originally shown the Duowa section by Zhou Liping and colleagues from the Desert Institute in Lanzhou. This work was supported by the Leverhulme Trust.

References

- Alley, R.B., Mayewski, P.A., Sowers, T., Stuiver, M., Taylor, K.C. and Clark, P.U. 1997: Holocene climatic instability. A prominent, widespread event 8200 yr ago. *Geology* 25, 483–86.
- An, Z.S., Porter, S.C., Kutzbach, J.E., Wu, X.H., Wang, S.M., Liu, X.D., Li, X.Q. and Zhou, W.J. 2000: Asynchronous Holocene optimum of the East Asian monsoon. *Quaternary Science Reviews* 19, 743–62.
- Basil, A. and Bush, G. 2001: Pacific sea surface temperature forcing dominates orbital forcing of the Early Holocene monsoon. *Quaternary Research* 55, 25–32.
- Berger, A. and Loutre, M.F. 1991: Insolation values for the climate of the last 10 million years. *Quaternary Science Reviews* 10, 297–317.
- Bond, G., Kromer, B., Beer, J., Muscheler, R., Evans, M.N., Showers, W., Hoffmann, S., Lotti-Bond, R., Hajdas, I. and Bonani, G. 2001: Persistent solar influence on north Atlantic climate during the Holocene. *Science* 294, 2130–36.
- deMenocal, P., Ortiz, J., Guilderson, T., Adkins, J., Sarnthein, M., Baker, L. and Yarusinsky, M. 2000: Abrupt onset and termination of the African Humid Period. Rapid climate responses to gradual insolation forcing. *Quaternary Science Reviews* 19, 347–61.
- Fleitmann, D., Burns, S.J., Mudelsee, M., Neff, U., Kramers, J., Mangini, A. and Matter, A. 2003: Holocene forcing of the Indian monsoon recorded in a stalagmite from Southern Oman. *Science* 300, 1737–39.
- Gagan, M.K., Hendy, E.J., Haberle, S.G. and Hantaro, W.S. 2004: Post-glacial evolution of the Indo-Pacific Warm Pool and El Niño–Southern Oscillation. *Quaternary International* 118–119, 127–43.
- Gasse, F. 2000: Hydrological changes in the African tropics since the Last Glacial Maximum. *Quaternary Science Reviews* 19, 189–211.
- Gasse, F. and van Campo, E. 1994: Abrupt post-glacial climate events in West Asia and North Africa monsoon domains. *Earth and Planetary Science Letters* 126, 435–56.
- Gasse, F., Tehet, R., Durand, A., Gibert, E. and Fontes, J.C. 1990: The arid humid transition in the Sahara and the Sahel during the last deglaciation. *Nature* 346, 141–46.
- Gasse, F., Arnold, M., Fontes, J.C., Fort, M., Gilbert, E., Huc, A., Bingyan, Li, Yuangang, Li, Qing, Liu, Mélières, F., van Campo, E., Fubao, Wang and Qingsong, Zang 1991: A 13,000-year climate record from western Tibet. *Nature* 353, 742–45.
- Gasse, F., Fontes, J.C., van Campo, E. and Wei, K. 1996: Holocene environmental changes in Bangong Co basin (Western Tibet). 4. Discussion and conclusions. *Palaeogeography, Palaeoclimatology, Palaeoecology* 120, 79–92.
- Ghil, M. 2002: Advanced spectral methods for climatic time series. *Reviews of Geophysics* 40, 41.
- Harrison, S.P., Jolly, D., Laarif, F., Abe-Ouchi, A., Dong, B., Herterich, K., Hewitt, C., Joussaume, S., Kutzbach, J.E., Mitchell, J., de Noblet, N. and Valdes, P. 1998: Intercomparison of simulated global vegetation distributions in response to 6 kyr BP orbital forcing. *Journal of Climate* 11, 2721–42.
- Huang, C.C., Zhou, J., Pang, J., Han, Y.P. and Hou, C.H. 2000: A regional aridity phase and its possible cultural impact during the Holocene Megathermal in the Guazhong Basin, China. *The Holocene* 10, 135–43.
- Huang, C.C., Pang, J., Huang, P., Hou, C. and Han, Y. 2002: High-resolution studies of the oldest cultivated soils in the southern Loess Plateau of China. *Catena* 47, 29–42.
- Jenny, H. 1941: *Factors of soil formation*. McGraw-Hill.
- Jolly, D., Harrison, S.P., Dammati, B. and Bonnefille, R. 1998: Simulated climate and biomes of Africa during the Late Quaternary. Comparison with pollen and lake status data. In Webb, T., III, editor, Late Quaternary climates. Data syntheses and model experiments. *Quaternary Science Reviews* 17, 629–57.
- Joussaume, S., Braconnot, J.F.B., Mitchell, J.E., Kutzbach, S.P., Harrison, I.C., Prentice, A.J., Broccoli, A., Abe-Ouchi, P.J., Bartlein, C., Taylor, K.E.P., Bonfils, B., Dong, J., Guiot, K., Herterich, C.D., Hewitt, D., Jolly, J.W., Kim, A., Kislov, A., Kitoh, A.F., Moutre, V., Masson, B., McAvaney, N., McFarlane, N., de Noblet, W.R., Peltier, J.Y., Peterschmitt, D., Pollard, D., Rind, J.F., Royer, M.E., Schlesinger, J., Syktus, S., Thompson, V., Valdes, G., Vettoretti, Webb, R.S. and Wyputta, U. 1999: Monsoon changes for 6000 years ago. Results of 18 simulations from the Paleoclimate Modelling Intercomparison Project (PMIP). *Geophysical Research Letters* 26, 859–62.
- Kitoh, A. and Murakami, S. 2002: Tropical Pacific climate at the mid-Holocene and the Last Glacial Maximum simulated by a coupled ocean–atmosphere general circulation model. *Paleoceanography* 17, art. no. 1047.
- Kutzbach, J., Guetter, P.J., Behling, P.J. and Delin, R. 1993: Simulated climatic changes. Results of the COHMAP climate-model experiments. In Wright, H.E., Jr, Kutzbach, J.E., Webb, T., III, Ruddiman, W.F., Paract, F.A. and Bartlein, P.J., editors, *Global climates since the Last Glacial Maximum*. University of Minnesota Press, 5–11.
- Liu, Z., Kutzbach, J. and Wu, L. 2000: Modelling climate shift of El Niño variability in the Holocene. *Geophysical Research Letters* 27, 2265–68.
- Liu, Z., Harrison, S.P., Kutzbach, J. and Otto-Bliesner, B. 2004: Global monsoons in the mid-Holocene and oceanic feedback. *Climate Dynamics* 22, 157–82.
- Maher, B.A., Thompson, R. and Zhou, L.P. 1994: Spatial and temporal reconstructions of changes in the Asian palaeomonsoon. A new mineral magnetic approach. *Earth and Planetary Science Letters* 125, 461–71.
- Maher, B.A. and Thompson, R. 1995: Palaeorainfall reconstructions from pedogenic magnetic susceptibility variations in the Chinese loess and paleosols. *Quaternary Research* 44, 383–91.
- 1999: Palaeomonsoons I: the palaeoclimatic record of the Chinese loess and paleosols. In Maher, B.A. and Thompson, R., editors, *Quaternary climates, environments and magnetism*. Cambridge University Press, 81–125.
- Maher, B.A., Alekseev, A. and Alekseeva, T. 2002a: Variation of soil magnetism across the Russian steppe. Its significance for use of soil magnetism as a palaeorainfall proxy. *Quaternary Science Reviews* 21, 1571–76.
- Maher, B.A., Hu, M., Roberts, H.M. and Wintle, A.G. 2002b: Holocene loess accumulation and soil development at the western edge of the Chinese Loess Plateau. Implications for magnetic proxies of palaeorainfall. *Quaternary Science Reviews* 22, 445–51.
- Marchant, R. and Hooghiemstra, H. 2004: Rapid environmental change in African and South American tropics around 4000 years before present: a review. *Earth Science Reviews* 66, 217–60.
- Morrill, C., Overpeck, J.T. and Cole, J.E. 2003: A synthesis of abrupt changes in the Asian summer monsoon since the last glaciation. *The Holocene* 13, 465–76.
- Moy, C.M., Seltzer, G.O., Rodbell, D.T. and Anderson, D.M. 2002: Variability of El Niño/Southern oscillation activity at millennial timescales during the Holocene epoch. *Nature* 420, 162–65.
- New, M., Hulme, M. and Jones, P. 2000: Representing twentieth-century space–time climate variability. Part II. Development of 1901–96 monthly grids of terrestrial surface climate. *Journal of Climate* 13, 2217–38.
- Núñez, L., Grosjean, M. and Cartajena, I. 2002: Human occupations and climate change in the Puna de Atacama, Chile. *Science* 298, 821–24.
- Overpeck, J., Anderson, D., Trumbore, S. and Prell, W. 1996: The southwest Indian monsoon over the last 18,000 years. *Climate Dynamics* 12, 213–25.
- Paillard, D., Labeyrie, L. and Yiou, P. 1996: Macintosh program performs time-series analysis. *Eos, Transactions of the American Geophysical Union* 77, 379.
- Pang, J.L., Huang, C.C. and Zhang, Z.P. 2003: Micromorphological and geochemical evidence of climate variations in the southern Loess Plateau of China during the last 10000 years. *Eurasian Soil Science* 36, 136–48.
- Porter, S.C., Hallet, B., Wu, X. and An, Z. 2001: Dependence of near-surface magnetic susceptibility on dust accumulation rate and precipitation on the Chinese Loess Plateau. *Quaternary Research* 55, 271–83.

- Rhodes, T.E., Fontes, J.-C., Kegin, W., Bertrand, P., Gibert, E., Melieres, F., Tucholka, P., Wang, Z., Gasse, F., Ruifen, L. and Cheng, Z.-Y. 1996: A late Pleistocene–Holocene lacustrine record from lake manas, Zunggar (northern Xinjiang, western China). *Palaeogeography, Palaeoclimatology, Palaeoecology* 120, 105–21.
- Roberts, H.M., Wintle, A., Maher, B.A. and Hu, M. 2001: Holocene loess accumulation rates in the western Loess Plateau, China, and a 2,500-year record of agricultural activity, revealed by OSL dating. *The Holocene* 11, 477–83.
- Shi, Y., Kong, Z., Wang, S., Tang, L., Wang, F., Yao, T., Zhao, X., Zhang, P. and Shi, S. 1993: Mid-Holocene climates and environments in China. *Global and Planetary Change* 7, 219–33.
- Street, F.A. and Grove, A.T. 1979: Global maps of lake-level fluctuations since 30,000 years ago. *Quaternary Research* 12, 83–118.
- Street-Perrot, F.A. and Harrison, S.A. 1984: Temporal variations in lake levels since 30,000 yr BP – an index of the global hydrological cycle. In Hansen, J.E. and Takahashi, T., editors, *Climate processes and climate sensitivity*. American Geophysical Union, 118–29.
- Stuiver, M., Braziunas, T.F., Grottes, P.M. and Zielinski, G.A. 1997: Is there evidence of solar forcing of climate in the GISP2 oxygen isotope record? *Quaternary Research* 48, 259–66.
- Texier, D., de Noblet, N. and Braconnot, P. 2000: Sensitivity of the African and Asian monsoons to mid-Holocene insolation and data-inferred surface changes. *Journal of Climate* 13, 164–81.
- Turney, C.S.M., Kershaw, A.P., Clemens, S.C., Branch, N., Moss, P.T. and Fifield, L.K. 2004: Millennial and orbital variations of El Niño/Southern Oscillation and high-latitude climate in the last glacial period. *Nature* 428, 306–10.
- Van Campo, E., Cour, P. and Huang, S. 1996: Holocene environmental changes in Bangong Co basin (Western Tibet). 2. The pollen record. *Palaeogeography, Palaeoclimatology, Palaeoecology* 120, 49–63.
- Verschuren, D., Briffa, K., Hoelzmann, P., Barber, K., Barker, P., Scott, L., Snowball, I. and Roberts, N. 2003: Holocene climate variability in Europe and Africa. a PAGES-PEP III time stream 1 synthesis. In Battarbee, R.W., Gasse, F. and Stickley, C.E., editors, *Past climate variability through Europe and Africa*. Kluwer, 1–15.
- Wang, L., Sarnthein, M., Erlenkeuser, H., Grimalt, J., Grootes, P., Helig, S., Ivanova, E., Kienast, M., Pelejero, C. and Pflaumann, U. 1999: East Asian monsoon climate during the Late Pleistocene. High-resolution sediment records from the South China Sea. *Marine Geology* 156, 245–84.
- Winkler, M.G. and Wang, P.K. 1993: The Late-Quaternary vegetation and climate of China. In Wright, H.E., Jr, Kutzbach, J.E., Webb, T., III, Ruddiman, W.F., Street-Perrott, F.A. and Bartlein, P.J., editors, *Global climates since the Last Glacial Maximum*. University of Minnesota Press, 221–64.
- Wright, H.E., Jr, Kutzbach, J.E., Webb, T., III, Ruddiman, W.F., Street-Perrott, F.A. and Bartlein, P.J., editors 1993: *Global climates since the Last Glacial Maximum*. University of Minnesota Press.
- Xiao, J., Nakamura, T., Lu, H.Y. and Zhang, G.Y. 2002: Holocene climate changes over the desert/loess transition of north-central China. *Earth and Planetary Science Letters* 197, 11–18.
- Yang, D.Y., Yu, G., Xie, Y.B., Zhan, D.J. and Li, Z.J. 2000: Sedimentary records of large Holocene floods from the middle reaches of the Yellow River, China. *Geomorphology* 33, 73–88.
- Yang, S. 1996: ENSO–snow–monsoon associations and seasonal–interannual predictions. *International Journal of Climatology* 16, 125–34.
- Zhang, H.C., Ma, Y.Z., Wunnemann, B. and Pachur, H.J. 2000: A Holocene climatic record from arid northwestern China. *Palaeogeography, Palaeoclimatology, Palaeoecology* 162, 389–401.
- Zhou, W.J., An, Z.S. and Head, M.J. 1994: Stratigraphic division of Holocene loess in China. *Radiocarbon* 36, 37–45.

Copyright of *Holocene* is the property of Arnold Publishers and its content may not be copied or emailed to multiple sites or posted to a listserv without the copyright holder's express written permission. However, users may print, download, or email articles for individual use.